ChemComm

COMMUNICATION

View Article Online
View Journal

Cite this: DOI: 10.1039/d6cc00888g

Received 10th February 2026,
Accepted 8th April 2026

DOI: 10.1039/d6cc00888g

rsc.li/chemcomm

Copper and manganese diazacalix[4]arene complexes: structural and cytotoxicity studies and use in ring opening polymerization of ε-caprolactone and δ-valerolactone

Azaria C. Razieh, †[a] Harry C. Sample, †[a] Emily B. Hobson,[b] Anja Mueller,[b] Timothy J. Prior[c] and Carl Redshaw *[bd]

From reactions of $M(OAc)_2{\cdot}nH_2O$ (M = Cu, Mn) or $Cu(NO_3)_2{\cdot}3H_2O$ with *p*-methyl-*N*,*N*′-dimethyldiazacalix[4]areneH_4 (*p*-MeLH_4) under aerobic conditions, rare examples of azacalixarene-3d-metal complexes were isolated. These, thermally stable non-toxic compounds (≤μM IC_{50} values) were screened as catalysts for the ring opening polymerization of the cyclic esters ε-caprolactone (ε-CL) and δ-valerolactone (δ-VL) affording low molecular weight cyclic or linear (H/OH end group) polymers. The Mn-based system exhibited the higher activity.

There is continued interest in the design of new catalyst systems capable of affording biodegradable polymers,[1] *via* the ring opening polymerization (ROP) of cyclic esters, as alternatives to petroleum-based products.[2] The use of earth abundant metals for such catalysis is also attracting interest,[3] and it is also desirable if the ancillary ligation allows for facile modification, in order that both catalytic activity and polymer properties can be controlled. Moreover, if such systems are to attract industrial interest, the catalyst system needs to exhibit low toxicity.

With this in mind, we have been investigating the combinations of earth abundant metals with the phenolic class of macrocycles known as calixarenes, and have reported a number of promising systems that are capable of the efficient ROP of cyclic esters.[4] Calixarenes not only have two rims that can be readily modified, but also the bridging group linking the phenols can take a number of forms. Typically, the bridge is a methylene ($-CH_2-$) group but calixarenes containing other bridges do exist, some of which exhibit the capability to interact with other metals present. Other bridging groups include thia (–S–),[5] sulfinyl (–SO–),[6] sulfonyl ($-SO_2-$),[6] dimethyleneoxa ($-CH_2OCH_2-$)[7] and aza ($-CH_2N(R)CH_2-$).[8] Other catalytic studies, for example α-olefin polymerization, have noted how changing the linkage of the calixarene can lead to enhanced catalytic performance.[9] Surprisingly the coordination chemistry of metalloazacalix[*n*]arenes is rather scant;[4i,8] a search of the CSD revealed less than 10 hits.[4i,10,11]

Copper and manganese are both 3d-elements with rich catalytic efficacy, both in biological and laboratory settings.[12] The toxicity of copper is, generally, lower than that of the heavier 4d- and 5d-transition metals,[13] and it is also one of the most abundant transition metals in the earth's crust.[14,15] Estimates from both the 1950's and 1960's suggest that manganese is 20 times more abundant. Worldwide production of each of these elements reached 20 million metric tonnes in 2023, as estimated by the U.S. Geological Survey.[16]

Given then the low cost and high abundance of these metals, combined with the lack of information on metalloazacalix[4]-arenes, we decided to probe the coordination chemistry of diazacalix[4]arene *p*-MeLH_4 (Chart 1) towards copper and manganese.

We have structurally characterized three new complexes (Chart 2), one of which (**2**) is the result of a copper catalysed ring cleavage, generating *p*-MeL^oH_5. The stability and toxicity of these complexes is also reported, together with the ability to act as catalysts for the ROP of ε-caprolactone and δ-valerolactone.

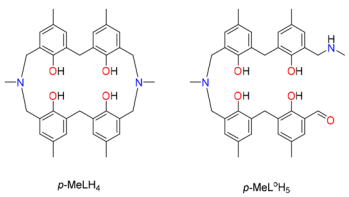

Chart 1 Azacalix[4]arene *p*-MeLH_4 and the ring-opened compound *p*-MeL^oH_5.

[a] *Department of Chemistry & Biochemistry, University of Hull, Hull, HU6 7RX, UK*
[b] *School of Chemistry, Pharmacy and Pharmacology, University of East Anglia, Norwich NR4 7TJ, UK*
[c] *Department of Chemistry, University of Liverpool, Crown Street, Liverpool, L69 7ZD, UK*
[d] *Department of Chemistry, Graduate School of Science, Tokyo Metropolitan University, 1-1 Minami Osawa, Hachioji, Tokyo, 192-0397, Japan. E-mail: credshaw@tmu.ac.jp*
† Both authors contributed equally to this work.

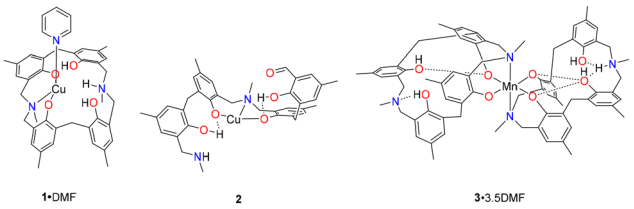

Chart 2 Complexes **1–3** reported herein.

Synthesis and structural studies. The ligand *p*-MeLH$_4$ was synthesized according to previous reports, utilizing Takemura's modifications to Burke's early dihydrobenzoxazine route.[17] Analytical data for this is provided in the SI (Fig. S19–S25). In our hands, we were able to generate >20 g of pure *p*-MeLH$_4$ from commercially available phenol dimers in less than a week.

Our route to the systems **1–3** utilized starting materials of suitable availability requiring little to no purification, nor anhydrous conditions or potential reactive (*e.g.* pyrophoric) species (*i.e.* all experiments were conducted open to air, with no protection from light, see SI). We note that Dalgarno, Brechin *et al.*,[18] have also reported an attractive route to manganese-based calix[4]arene systems which were found to behave as single molecule magnets.

Copper complexes. Our entry point into this chemistry was *via* the reaction of Cu(NO$_3$)$_2$·3H$_2$O with *p*-MeLH$_4$ in DMF/MeOH in the presence of pyridine. Work-up led to the formation of dark blocks of [Cu(*p*-MeLH$_3$)(Py)(NO$_3$)]·DMF (**1**·DMF). The molecular structure is shown in Fig. 1 with selected bond lengths and angles given in the caption; alternative views in the SI. The structure of **1** is clearly established but the quality of the fit to the observed data is rather poor. This is a consequence of the poor quality of the crystals examined and this sample seems to be pathologically twinned.

The structure presents a copper(II) complex consisting of a monodeprotonated ligand, *i.e.* *p*-MeLH$_3$, with the charge balanced by the nitrate counter-ion. The coordination environment around the copper is that of a *trans*-[Cu^{II}O$_2$N$_2$] type, consisting of two phenoxide-oxygen atoms, one of the 3° amine aza-bridges, and completed by the pyridine. The geometry about the copper is best described as an extremely flattened tetrahedron (for details of metal coordination of this and other complexes see SI). Both Cu–O bonds are considerably shorter than Cu–N bonds; Cu1–O1 and Cu–O4 distances are 1.893(9) Å and 1.887(9) Å respectively compared with 2.015(12) Å and 2.053(12) Å for Cu1–N1 and Cu1–N3. Whilst two phenoxides are seen to have been deprotonated, the 3° amine aza-bridge has been protonated. The two coordinating phenoxide oxygen atoms are also seen to be participating in intramolecular O–H···O interactions with the other phenolic-OH motifs within the ligand.

Through the synthesis of multiple batches of these complexes, we observed a second polymorph of **1**, structurally similar to the first (see SI for discussion).

We continued our studies *via* reaction of Cu(OAc)$_2$·H$_2$O with *p*-MeLH$_4$ in DMSO/MeOH in the presence in pyridine. Work-up and prolonged standing led to the formation of green prisms of [Cu(*p*-MeL^{O}H$_3$)]$_2$ (**2**). The molecular structure is shown in Fig. 2 with selected bond lengths and angles given in the caption; alternative views are provided in the SI.

Again, the coordination environment about the copper can be described as a flattened tetrahedron with *trans*-[Cu^{II}O$_2$N$_2$] type coordination from two phenoxide-oxygen atoms, and the 3° amine from the aza-bridge between them. The final coordination however arises from a 2° amine of the ligand of an adjacent molecule. The structure presents, again, protonated amine bridges along with intramolecular O–H···O interactions. As a result of these interactions, **2** exists as helically structured dimers with the Cu–Cu axis oriented perpendicular to the crystallographic *b*-direction.

The coordination chemistry of copper is particularly rich as exemplified by its performance in a variety of catalytic transformations.[12,19] In this attempt to generate copper azacalix[4]arene complexes, we have observed an oxidative ring opening of *p*-MeLH$_4$ cleaving one of the C$_{sp^3}$–N$_{Aza}$ bonds (Fig. 2), generating

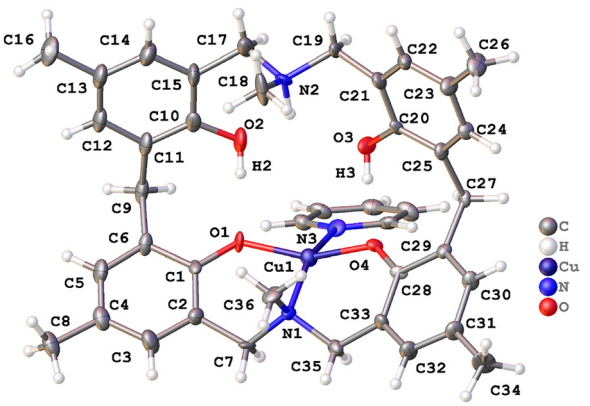

Fig. 1 Asymmetric unit of [Cu(*p*-MeLH$_3$)(Py)(NO$_3$)]·DMF, (1·DMF). Atoms represented as thermal ellipsoids at the 50% probability level. NO$_3^-$ counterion and DMF omitted for clarity. Image generated in Olex2.[20] Py = C$_5$H$_5$N. Selected bond lengths (Å) and angles (°): Cu1–O1 1.402(19), Cu1–O4 1.419(17), Cu1–N1 2.015(12), Cu1–N3 2.053(12); O1–Cu1–O4 156.1(4), N1–Cu1–N3 156.7(5).

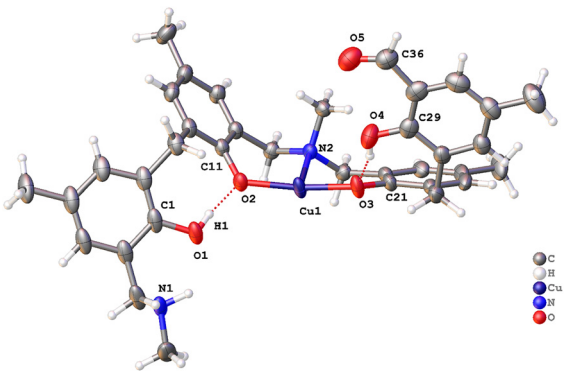

Fig. 2 Asymmetric unit of [Cu(*p*-MeL^{O}H$_3$)]$_2$ (**2**). Atoms represented as thermal ellipsoids at the 50% probability level. Image generated in Olex2.[20] Selected bond lengths (Å) and angles (°): Cu1–O2 1.9063(16), Cu1–O3 1.9125(17), Cu1–N2 2.0166(18), Cu1–N1_$1 2.221(2); O2–Cu1–O3 165.17(8), N2–Cu1–N1_$1 89.24(8). $1 = 1 − *x*, *y*, 1/2 − *z*.

an open chain ligand containing both salicylaldehyde and 2° amine motifs (*p*-MeL^{O}H$_5$). Similar cleavages have been observed in a wide variety of systems employing both Cu^{I} and Cu^{II} salts in the presence of C_{sp^3}–N_{sp^3} bonds.[19c–f] Such a transformation highlights a susceptibility in the azacalix[*n*]arene scaffold that had not been previously considered and may have ramifications in further generation of copper azacalix[*n*]arene systems.

Manganese complex. We continued our studies *via* reaction of Mn(OAc)$_2$·4H$_2$O with *p*-MeLH$_4$ in DMF/MeOH in the presence of triethylamine. Work-up led to the formation of black prisms of [Mn(*p*-MeLH$_2$)(*p*-MeLH$_3$)]·3.5DMF (**3**·3.5DMF). The molecular structure is shown in Fig. 3 with selected bond lengths and angles given in the caption; alternative views are provided in the SI.

The structure presents with two ligands coordinating the manganese ion in similar fashions, with only the intra-ligand H-bonding pattern to differentiate them. Analysis of the distorted octahedral manganese environment reveals a *trans*-[MnN$_2$O$_4$] system, with four phenoxide oxygen atoms taking up the equatorial plane, and an elongation along the N–Mn–N axis. Whilst the starting material for this synthesis was Mn^{II}, the crystallographic results are consistent with a Mn^{III} centre. Furthermore, our own measurements of paramagnetic susceptibility *via* the Evans NMR Method indicated $\mu_{eff} = 4.82\mu_B$, further agreement with a Jahn–Teller distorted octahedral Mn^{III} centre.

Ring opening polymerization (ROP). Complexes **1–3** and the parent azacalix[4]arene *p*-MeLH$_4$ were screened for their ability to act as catalysts for the ROP of the cyclic esters ε-caprolactone (ε-CL) and δ-valerolactone (δ-VL) in toluene at 110 °C (**2** only) and as melts (150 °C) with and without benzyl alcohol (BnOH) present. Given the interest in metal-free ROP,[21] the parent diazacalix[4]arene *p*-MeLH$_4$ was also screened. The results are presented in Table 1.

ε-Caprolactone. When employed as melts, in the absence of BnOH, **1** and **3** (entries 1 and 4, Table 1) exhibited near quantitative conversion of ε-CL affording low to moderate molecular weight (M_n) polymers with good control (dispersity $Đ \leq 1.25$). In the case of **2**, only when employed in toluene in the presence of BnOH (entry 3, Table 1) was high conversion observed. In all cases, observed molecular weights (M_n) were lower than calculated values, suggesting the presence of transesterification processes. Kinetic profiles (Fig. 4 and Fig. S6) revealed that the manganese system **3** was far more active the copper systems **1** and **2**, with the former exhibiting an induction period which results in a curved profile. This is thought to be due to slow insertion; all systems operate *via* a coordination/insertion mechanism. In MALDI-ToF spectra (Fig. S7–S10, SI), both linear (end group H/OH) and cyclic products are observed mostly as potassium adducts. The parent *p*-MeLH$_4$ exhibited only negligible activity (entry 5, Table 1).

Table 1 ROP of ε-CL and δ-VL using **1–3** and *p*-MeLH$_4$

Entry	Cat.	[M]:[Cat]:BnOH	Conv.[a] (%)	Mn[bc] (Da)	Mn$_{Cal}$[c] (Da)	$Đ$[d]
ε-CL						
1	**1**	500:1:0	>99	4630	31 650	1.25
2	**2**	500:1:0	51	6730	16 310	1.19
3[d]	**2**	500:1:1	>99	4300	31 650	1.04
4	**3**	500:1:0	>99	7530	31 650	1.02
5	*p*-MeLH$_4$	500:1:0	<1	—	—	—
δ-VL						
6	**1**	500:1:0	>99	5130	28 260	1.20
7	**2**	500:1:0	85	5230	24 320	1.17
8	**2**	500:1:1	>99	4340/2030*	28 260	1.08/1.02
9	**3**	500:1:0	32	7870	91 60	1.08
10	*p*-MeLH$_4$	500:1:0	>99	1190/710	28 260	1.02/1.03

Conditions: solvent-free, T = 150 °C, 24 h, under air. [a] Determined by ^{1}H NMR spectroscopy on the crude reaction mixture. [b] From GPC. [c] Values corrected considering Mark–Houwink factor (0.56 for ε-CL; 0.57 for δ-VL) from polystyrene standards in THF.[22] [d] Conducted in toluene at 110 °C.

δ-Valerolactone. For the ROP of δ-VL, systems employing **1** and **2** exhibited good conversions (≥85%) when employed as melts (entries 6 and 7, Table 1) affording polymers of similar molecular weight (M_n, 5130–5230 Da), with good control ($Đ \leq$ 1.20). When **2**/BnOH was used in toluene (entry 8, Table 1), bimodal behaviour was observed. For **3** as a melt, the conversion was much lower (32%), however higher molecular weight (M_n) polymer was formed (7870 Da) with better control ($Đ$ 1.08). In this case, the parent *p*-MeLH$_4$ exhibited near quantitative conversion (entry 10, Table 1) with bimodal behaviour and affording lower molecular weight products. As for PCL, the

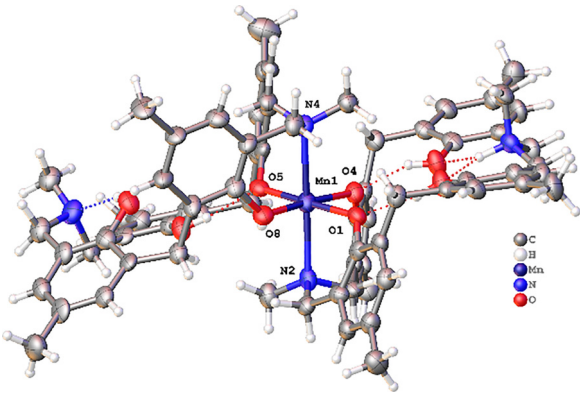

Fig. 3 Asymmetric unit of [Mn(*p*-MeLH$_2$)(*p*-MeLH$_3$)]·3.5DMF (**3**·3.5DMF). DMFs have been omitted for clarity. Atoms represented as thermal ellipsoids at the 50% probability level. Image generated in Olex2.[20] Selected bond lengths (Å) and angles (°): Mn1–O1 1.997(8), Mn1–O4 1.937(4), Mn1–O5 1.973(5), Mn1–O8 1.880(4), Mn1–N2 2.296(6), Mn1–N4 2.321(6); O1–Mn1–O4 86.0(2), O1–Mn1–O3 176.79(19), N2–Mn1–N4 176.0(2).

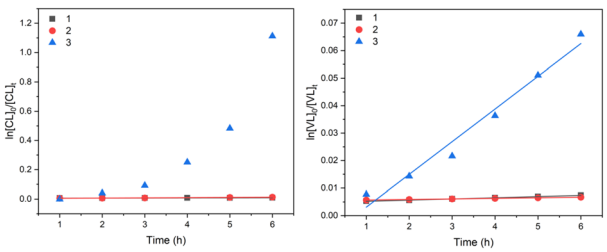

Fig. 4 Kinetic profiles using **1–3** (left PCL, right PVL).

Table 2 Cytotoxicity of **1–3** using MCF-7 and PC3 cell lines[24]

Cell line	**1**·DMF	**2**	**3**·3.5DMF
MCF-7	14.41 μM ± 5.57	12.17 μM ± 2.11	No effect
PC3	4.09 μM ± 1.05	43.71 μM ± 22.72	3.55 μM ± 0.45

kinetic profiles revealed the order **3** > **1** ≈ **2** under the conditions employed. In this case, the profile for **3** was more linear. MALDI-ToF spectra (Fig. S12 and S13, SI) revealed the presence of cyclic and linear (H/OH end groups) polymers mostly as sodium adducts.

ROP results are compared *versus* the industry favoured catalyst [Sn(Oct)$_2$] in the SI.[23]

The thermostability of the complexes at the polymerization temperature (110 °C in toluene, 150 °C as melts) was checked by TGA. Prior to reaching the polymerization temperature, only the copper complexes exhibited a slight weight loss (~10% for **1**·DMF, ~5% for **2**), which is attributed to the loss of crystallization solvent (DMF), see Fig. S40, SI. In the case of **1**·DMF, increasing the temperature beyond 150 °C led to significant weight loss (~50%) and is attributed to decomposition (loss of calixarene ligand), followed by loss of pyridine leaving residual inorganic salts.

*Cytotoxicity of **1**·DMF, **2**, and **3**·3.5DMF*. Given such polymers are often deployed in medical applications, it is critical to be aware of any possible toxicity that is present as a result of catalyst contamination. Given this, we have evaluated them *via* MTS assays of the three complexes and the parent calixarene against two cell lines as to ascertain their IC_{50} values (Table 2).

The parent compound (*p*-MeLH$_4$) showed no toxicity across both cell lines tested, however there was some activity with all three compounds in the PC3 cells, with **3** being the most potent, but only **1** and **2** seemed to have activity in the MCF-7 cells. Overall, the activity is quite low, only showing toxicity above micromolar concentration.

In conclusion, we have structurally characterized rare examples of metal azacalix[4]arene complexes. In one case, an interesting ring opening of the calixarene was observed. Screening of these complexes for the ROP of the cyclic esters δ-valerolactone (δ-VL) and ε-caprolactone (ε-CL) revealed the Mn derivative to be the most active, with all systems forming either cyclic or linear (H/OH end groups) polymers. Further azacalixarene coordination chemistry is now in progress.

Conflicts of interest

There are no conflicts to declare.

Data availability

The data supporting this article have been included as part of the electronic supplementary information (SI). Supplementary information: full experimental details for complex synthesis and ROP studies. See DOI: https://doi.org/10.1039/d6cc00888g.

CCDC 2545706–2545709 contain the supplementary crystallographic data for this paper.[25a–d]

Acknowledgements

We thank the University of Hull for a PhD Scholarship to ACR. The EPSRC National Crystallographic Service Centre at Southampton is thanked for data. CR also thanks the EPSRC (grant EP/X01374X/1) for financial support.

References

1 (*a*) X. Zhang, M. Fevre, G. O. Jones and R. M. Waymouth, *Chem. Rev.*, 2018, **118**, 839–885; (*b*) S. S. Panchal and D. V. Vasava, *ACS Omega*, 2020, **5**, 4370–4379; (*c*) A. Samir, F. H. Ashour, A. A. A. Hakim and M. Bassyouni, *npj Mater. Degrad.*, 2022, **6**, 68; (*d*) M. Kuang, B. Li, L. Zhou, Z. Huang, J. Wu, S. Wang and J. Yang, *Angew. Chem., Int. Ed.*, 2025, **64**, e202422357.
2 (*a*) I. Nifant'ev and P. Ivchenko, *Molecules*, 2019, **24**, 4117; (*b*) F. Naz, R. M. Abdur, F. Mumtaz, M. Elkadi and F. Verpoort, *Appl. Organomet. Chem.*, 2023, **37**, e7296; (*c*) L. Wang, Y. Liu, Y. Shen and Z. Li, *Polym. Chem.*, 2014, **15**, 3832–3846; (*d*) R. Morodo, D. M. Dumas, J. Zhang, K. H. Lui, P. J. Hurst, R. Bosio, L. M. Campos, N. H. Park, R. M. Waymouth and J. L. Hedrick, *ACS Macro Lett.*, 2024, **13**, 181–188; (*e*) Y. Pan, M. Hao, X. Li, Y. Meng, X. Kang, G. Zhang, X. Sun, X.-Z. Song, L. Zhang and Y.-M. So, *Inorg. Chem.*, 2025, **64**, 530–544.
3 (*a*) D. Wang and D. Astruc, *Chem. Soc. Rev.*, 2017, **46**, 816–854; (*b*) B. M. Hockin, C. Li, N. Robertson and E. Zysman-Colman, *Catal. Sci. Technol.*, 2019, **9**, 889–915; (*c*) R. M. Bullock, J. G. Chen, L. Gagliardi, P. J. Chiriki, O. K. Farha, C. H. Hendon, C. W. Jones, J. A. Keith, J. Klosin, S. D. Minteer, R. H. Morris, A. T. Radosevich, T. Rauchfuss, N. A. Strotman, A. Vojvodic, T. R. Ward, J. Y. Yang and Y. Surendranath, *Science*, 2020, **369**, eabc3183; (*d*) P. J. Chirik, K. M. Engle, E. M. Simmons and S. R. Wisniewski, *Org. Process Res. Dev.*, 2023, **27**, 1160–1184; (*e*) K. M. P. Wheelhouse, R. L. Webster and G. L. Beutner, *Org. Process Res. Dev.*, 2023, **27**, 1157–1159.
4 (*a*) Z. Sun, Y. Zhao, O. Santoro, M. R. J. Elsegood, E. V. Bedwell, K. Zahra, A. Walton and C. Redshaw, *Catal. Sci. Technol.*, 2020, **10**, 1619–1639; (*b*) T. Xing, C. Jiang, M. R. J. Elsegood and C. Redshaw, *Inorg. Chem.*, 2021, **60**, 15543–15556; (*c*) C. Redshaw, *Dalton Trans.*, 2016, **45**, 9018–9030; (*d*) C. Redshaw, *Dalton Trans.*, 2025, **54**, 7146–7166; (*e*) D. M. Homden and C. Redshaw, *Chem. Rev.*, 2008, **108**, 5086–5130; (*f*) O. Santoro, M. R. J. Elsegood, S. J. Teat, T. Yamato and C. Redshaw, *RSC Adv.*, 2021, **11**, 11304–11317; (*g*) T. Xing, J. W. A. Frese, M. Derbyshire, M. A. Glenister, M. R. J. Elsegood and C. Redshaw, *Dalton Trans.*, 2022, **51**, 11776–11786; (*h*) H. J. S. Banks, J. W. A. Frese, M. R. J. Elsegood and C. Redshaw, *Chem. Commun.*, 2024, **60**, 304–307; (*i*) T. Xing, T. J. Prior, K. Chen and C. Redshaw, *Dalton Trans.*, 2021, **50**, 4396–4407; (*j*) T. Xing, T. J. Prior, M. R. J. Elsegood, N. V. Semikolenova, I. E. Soshinikov, K. Bryliakov, K. Chen and C. Redshaw, *Catal. Sci. Technol.*, 2021, **11**, 624–636.
5 (*a*) N. Morohashi, F. Narumi, N. Iki, T. Hattori and S. Miyano, *Chem. Rev.*, 2006, **106**, 5291–5316; (*b*) R. Kumar, Y. O. Lee, V. Bhalla, M. Kumar and J. S. Kim, *Chem. Soc. Rev.*, 2014, **43**, 4824–4870.
6 N. Iki, H. Kumagai, N. Morohashi, K. Ejima, M. Hasegawa, S. Miyanari and S. Miyano, *Tetrahedron Lett.*, 1998, **39**, 7559–7562.
7 K. Cottet, P. M. Marcos and P. J. Cragg, *Beilstein J. Org. Chem.*, 2012, **8**, 201–226.
8 H. Takemura, *Molecules*, 2021, **26**, 4885.
9 C. Redshaw, M. A. Rowan, L. Warford, D. M. Homden, A. Arbaoui, M. R. J. Elsegood, S. H. Dale, T. Yamato, C. P. Casas, S. Matsui and S. Matsuura, *Chem. – Eur. J.*, 2007, **13**, 1090–1107.
10 (*a*) P. Thuery, M. Nierlich, J. Vicens, B. Masci and H. Takemura, *Eur. J. Inorg. Chem.*, 2001, 637–643; (*b*) P. Thuéry, M. Nierlich, J. Vicens and H. Takemura, *Polyhedron*, 2000, **19**, 2673–2678.
11 C. R. Groom, I. J. Bruno, M. P. Lightfoot and S. C. Ward, *Crystallogr., Sect. B*, 2016, **72**, 171–179.
12 (*a*) R. Trammell, K. Rajabimoghadam and I. Garcia-Bosch, *Chem. Rev.*, 2019, **119**, 2954–3031; (*b*) T. Tsang, C. I. Davis and D. C. Brady, *Curr. Biol.*, 2021, **31**, R421–R427; (*c*) R. A. Layfield, *Chem. Soc. Rev.*, 2008, **37**, 1098–1107; (*d*) L. Li and X. Yang, *Oxid. Med. Cell. Longevity*, 2018, **2018**, 7580707.

13 K. S. Egorova and V. P. Ananikov, *Organometallics*, 2017, **36**, 4071–4090.
14 K. S. Egorova and V. P. Ananikov, *Angew. Chem., Int. Ed.*, 2016, **55**, 12111–12542.
15 (*a*) M. Fleischer, *J. Chem. Educ.*, 1954, **31**, 446–455; (*b*) S. R. Taylor, *Geochim. Cosmochim. Acta*, 1964, **28**, 1273–1285.
16 (*a*) US Geological Survery, Mineral Commodity Summaries, https://pubs.usgs.gov/periodicals/mcs2024/mcs2024-copper.pdf, (accessed December 2025); (*b*) US Geological Survery, Mineral Commodity Summaries https://pubs.usgs.gov/periodicals/mcs2024/mcs2024-manganese.pdf, (accessed December 2025).
17 (*a*) H. Takemura, A. Takahashi, H. Suga, M. Fukuda and T. Iwanaga, *Eur. J. Org. Chem.*, 2011, 3171–3177; (*b*) W. J. Burke, *J. Am. Chem. Soc.*, 1949, **71**, 609–612; (*c*) W. J. Burke, J. L. Bishop, E. L. Mortensen Glennie and W. N. Bauer Jr., *J. Am. Chem. Soc.*, 1965, **30**, 3423–3427.
18 G. Karotsis, S. J. Teat, W. Wernsdorfer, S. Piligkos, S. J. Dalgarno and E. K. Brechin, *Angew. Chem., Int. Ed.*, 2009, **48**, 8285–8288.
19 (*a*) D.-I. Tzaras, M. Gorai, T. Jacquemin, T. Arndt, B. M. Zimmermann, M. Breugst and J. F. Teichert, *J. Am. Chem. Soc.*, 2025, **147**, 1867–1874; (*b*) J. Li, Z. Liu, P. Liu and P. Sun, *Org. Biomol. Chem.*, 2016, **14**, 7018–7023; (*c*) J. B. Roque, Y. Kuroda, L. T. Göttemann and R. Sarpong, *Nature*, 2018, **564**, 244–248; (*d*) T. Nagakubo, T. Kumano, T. Ohta, Y. Hashimoto and M. Kobayashi, *Nat. Commun.*, 2019, **10**, 413; (*e*) G. Cocquet, C. Ferroud and A. Guy, *Tetrahedron*, 2000, **56**, 2975–2984; (*f*) W. Li, W. Liu, D. K. Leonard, J. Rabeah, K. Junge, A. Brückner and M. Beller, *Angew. Chem., Int. Ed.*, 2019, **58**, 10693–10697.
20 O. V. Dolomanov, L. J. Bourhis, R. J. Gildea, J. A. K. Howard and H. Puschmann, *J. Appl. Cryst.*, 2009, **42**, 339–341.
21 A. P. Dove, *ACS Macro Lett.*, 2012, **1**, 1409–1412.
22 (*a*) C.-H. Huang, F.-C. Wang, B.-T. Ko, T.-L. Yu and C.-C. Lin, *Macromolecules*, 2001, **34**, 356–361; (*b*) M. Save, M. Schappacher and A. Soum, *Macromol. Chem. Phys.*, 2002, **203**, 889–899.
23 T. J. Prior and C. Redshaw, *Catalysts*, 2025, **15**, 261.
24 Cell lines were purchased from ATCC.
25 (*a*) CCDC 2545706: Experimental Crystal Structure Determination, 2026, DOI: 10.5517/ccdc.csd.cc2rg0kt; (*b*) CCDC 2545707: Experimental Crystal Structure Determination, 2026, DOI: 10.5517/ccdc.csd.cc2rg0lv; (*c*) CCDC 2545708: Experimental Crystal Structure Determination, 2026, DOI: 10.5517/ccdc.csd.cc2rg0mw; (*d*) CCDC 2545709: Experimental Crystal Structure Determination, 2026, DOI: 10.5517/ccdc.csd.cc2rg0nx.